J Mater Sci
DOI 10.1007/s10853-011-5743-x

Prediction of the long-term behaviour of high modulus fibres using the stepped isostress method (SSM)

Ioannis P. Giannopoulos · Chris J. Burgoyne

Received: 31 March 2011 / Accepted: 23 June 2011

Abstract A new accelerated technique, called the stepped isostress method (SSM), is presented that allows accelerated testing of materials to determine their creep response, and in particular, their creep-rupture behaviour. The approach in SSM testing is similar to the more familiar stepped isothermal method (SIM) but the acceleration is now obtained by increasing the stress in steps rather than stepping the temperature. Additional stress provides energy to the system in an analogue of the effect of heat in SIM. This method relies on the time–stress superposition concept. Various theories, assumptions and the different steps of the method are described in detail. This method is advantageous when compared with SIM because there is no need to use elevated temperatures, which may affect the chemical properties of the tested materials. The applicability of this method is investigated. The paper presents testing on Kevlar 49 yarns using SSM. The resulting creep curves and rupture times are compared with those obtained from SIM and conventional creep testing carried out in the past. The results show good correlation between the three test methods. The ability to carry out reliable creep tests in a reasonable time at low stress levels allows a designer to have much more confidence in the data for creep-rupture behaviour for fibres and allows confident prediction of structural lifetimes.

I. P. Giannopoulos (✉)
Department of Architectural Engineering,
National Technical University of Athens, Athens, Greece
e-mail: igianno@cantab.net

C. J. Burgoyne
Department of Engineering, University of Cambridge,
Cambridge, UK
e-mail: cjb19@cam.ac.uk

Introduction

Because of their good tensile properties, low weight and lack of corrosion, aramid fibres have potential for use in many structural engineering applications such as tendons in prestressed concrete, stay cables in bridges and ropes in marine industry. However, required structural lifetimes can be as high as 120 years, and concern about creep-rupture phenomenon at high stress levels is an issue. Since the fibres are so expensive, there is an economic cost to providing extra material, and lack of certainty about predictions leads to excessive caution. It has been proposed that a life span of about 120 years is possible if the tendons are subjected only to 50% of the short-term strength [1, 2], while Gerritse and Taerwe [3] proposed limiting the initial stress in prestressing elements to 55% of the short-term strength. Even the manufacturers provide a large range of time-to-failure predictions when fibres are subjected to constant loads. The work presented here is one part of a much larger programme to determine the long-term properties of these fibres, and describes one of the test methods that were developed [4, 5]. One important aspect of this study is that all tests were carried out on the same materials, in the same grips to avoid differences in handling techniques, and also using the same size elements (1,000 filament yarns) to avoid complications due to bundle effects.

Many creep-rupture models [3, 6–15] have been proposed to predict the long-term creep-rupture behaviour of aramid fibres. However, these models are usually based on test data obtained at high load levels (>60% breaking load), when creep failures can be expected in a short period of time. For lower stress levels, extrapolations are used but the degree of extrapolation and the lack of test data introduce many uncertainties, so very large safety factors are applied for engineering design. Engineers are currently

Published online: 07 July 2011

forced to use low allowable stresses, resulting in significant economic disincentive. Less suitable materials are used simply because there is more confidence about their long-term properties.

As an alternative to extrapolation, accelerated creep-rupture testing can be carried out at low stress levels, in such a way that the long-term creep and creep-rupture properties can be determined within shorter time scales. The creep rate is accelerated, thus reducing the time needed for a given amount of creep to occur; failure of the specimen can then take place in practical timescales.

The creep rate of aramid fibres is influenced by many factors, such as temperature, humidity, physical ageing, damage, pressure, solvent concentration, strain and stress. Amongst these, temperature and stress are the most important for load-bearing polymeric materials [16].

Two accelerated methods make use of the effect of temperature to accelerate the creep rate. Using the time temperature superposition principle (TTSP), which usually assumes that creep is a thermally activated process, multiple specimens are tested under a constant load at different temperatures resulting in separate plots of creep strain versus log (time) at different temperatures. A reference temperature is then selected, usually close to ambient, and all individual curves are shifted along the log (time) axis to compensate for the different temperatures. By applying the principle of superposition a creep master curve is produced.

The second temperature-accelerated method is the stepped isothermal method (SIM) which was first used by Thornton et al. [17] to predict the long-term creep behaviour of geogrids in soil reinforcement applications. Later, Alwis and Burgoyne [18] applied this method to high modulus yarns. SIM involves loading a single specimen under a constant load. The temperature is then increased in a step-wise fashion, either until sufficient creep has occurred or the specimen fails. By applying a series of corrections, which account for the stepping of the temperature and the different degrees of creep at each stage, a single response curve, known as the master curve, is obtained which predicts the long-term behaviour. SIM testing relies of knowledge of an activation energy which has to be constant at all temperatures to show that the same creep mechanism is occurring.

Acceleration by changing the temperature works because energy is supplied to overcome the resistance to creep, but that energy can also be applied by increased stress. This effect has also received attention in recent years; the time–stress superposition concept (TSS) has been used to predict the creep behaviour of various polymeric materials. Lai and Bakker [19] performed creep tests on polyethylene specimens at various stress levels and at ambient temperature, and constructed a master curve at a reference stress using the time–stress superposition principle (TSSP). Hadid et al. [20] carried out creep tests on fibre glass reinforced polyamide specimens at various stress levels; the duration of each test was 30 min and by combining the results they constructed a smooth master curve at a reference stress. Jazouli et al. [21] studied the creep behaviour of polycarbonate by testing various specimens at room temperature and under various sustained loads for only 1 h. They then used these to construct a smooth master curve for 1 year. By analogy with the activation energy, where heat provides the energy needed for creep to occur, TSS assumes that stress can supply energy. This leads to the concept of an activation volume that will be described later.

By taking into account the combined effect of temperature and stress on the creep of viscoelastic materials, long-term creep deformations can be predicted. This method is based on the time–temperature–stress superposition concept and involves testing different specimens at various temperatures and stresses. First, the time–temperature principle is applied to produce master curves at various stress levels at a selected reference temperature. The time–stress principle is then applied to these master curves to get the final master curves at a given stress and temperature level. Ma et al. [22] and Luo and Wang [23] investigated the creep behaviour of carbon fibre reinforced polyetherketone and poly(methyl methacrylate), respectively by testing specimens under various temperatures and stresses.

Based on the methods described above, a different accelerated method, called the stepped isostress method (SSM), is proposed here to predict the long-term creep behaviour of Kevlar 49. A similar method was applied in the past by Farquhar et al. [24] to develop the creep-rupture properties of single IM6 carbon fibres, albeit without focusing on creep itself, and using a power-law (Weibull stress vs. lifetime) framework.

Description of the stepped isostress method (SSM)

The method involves loading a single specimen, instead of the many specimens required by TSSP. This single specimen is subjected to a step-wise increase in stress (similar to the isothermal approach, which used temperature steps) at a constant temperature (Fig. 1). These elevated stresses will be referred to as *accelerating stresses*, to distinguish them from the *reference stress* at which it is desired to construct the creep master curve. In the study that follows, the reference stress is always the initial stress on the yarn, but this need not be the case. At each stress step a creep curve (strain vs. time) is obtained; these can be adjusted to compensate for the different stress levels and a creep master curve at a reference stress level is produced. A creep–rupture point can then be determined as the very last point of each creep master curve. As with a SIM test, four

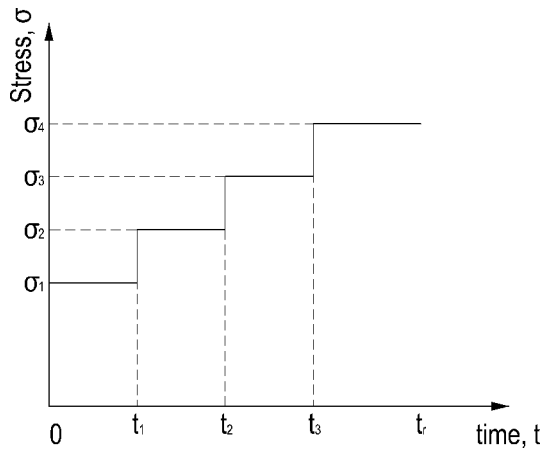

Fig. 1 SSM—a series of timed isostress exposures at elevated stress levels

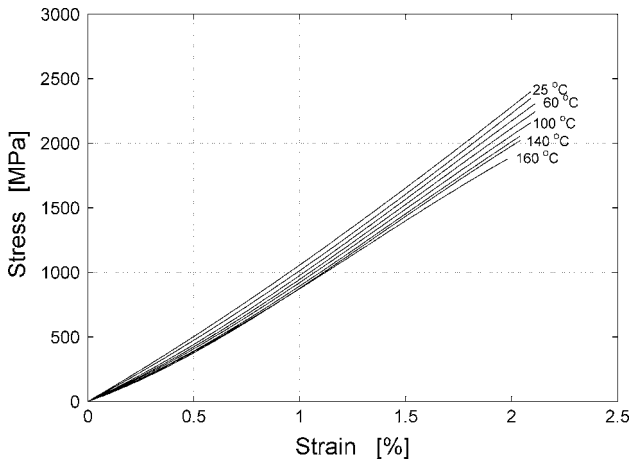

Fig. 2 Average stress versus strain curves using a mechanical strain gauge at all temperatures for Kevlar 49

adjustments are required (initial vertical adjustment, vertical shifting, rescaling, horizontal shift) to obtain the final master curve; details are given below.

The use of a single specimen minimises concerns about specimen variability and handling effects; TSSP needs more specimens and more handling. SSM can be automated and takes less time than TSSP, so offers several advantages.

Adjustments required

The key to the SSM method is the adjustments to the raw data that is obtained during the tests. Four such adjustments are needed.

Initial vertical adjustment

It is inevitable when testing fibres that a small amount of slack will be introduced and there will also be jaw effects. It is essential that these are eliminated because they can have a significant effect on the apparent creep rates.

According to Ericksen's work [25, 26], during a tensile or creep experiment, the loading strain rate significantly affects the yarns strength and modulus; hence it is critical to use a sensible strain rate. A rate of 1% of the nominal gauge length of the specimen per minute was recommended by the test machine manufacturer and this was adopted here. Thus, for a nominal length equal to 350 mm, a strain rate of 3.5 mm/min is used.

The specimen will be subjected to a constant temperature and then loaded to the desired first stress level using constant strain rate. It is essential to know accurately the expected strain immediately after first loading so that slack and jaw effects can be eliminated. Thus, a set of tensile tests are first carried out to determine the initial stress–strain curves at different temperatures, using standard procedures [4, 27] (Fig. 2). The strain as measured in the SSM test is thus adjusted by a constant offset to ensure that the strain as measured matches the value expected. Each test will give a slightly different value of strain just after loading, but after this adjustment, all strain versus time curves will have the initial strain equal to the accurate value. This is shown schematically in Fig. 3a.

Vertical shifting

At each stress jump an immediate increase in strain can be expected due to the elasticity of the fibre. These are shown schematically in Fig. 3a when the stress changes from σ_1 at A to σ_2 at B. Since the stress jump is almost instantaneous, there is no additional creep strain between A and B. The creep curve at stress σ_2 after the jump must be *shifted vertically* to remove the elastic strain, as shown in Fig. 3b, so that the final master curve is a purely creep curve. If the elastic modulus of the material was not affected by creep, it would be possible to compute the increase in strain as the stress increased σ_1 to σ_2 from the stress versus strain curve in Fig. 1. However, Giannopoulos [4] showed that the elastic modulus increases after a period of creep so this method was not applied here. Alternatively, the vertical shift can be determined graphically, so that the last point before the jump coincides with the first point after the jump. This is shown schematically in Fig. 3b. This method deals with the real elastic strain of each test, rather than a mean elastic strain obtained from tensile tests.

Rescaling

The curve that results from the vertical shift contains the creep results from elements of creep tests carried out at several different load levels. In Fig. 3b, the curve OA is at one load level, and B_1C_1 at a higher level. It is necessary to

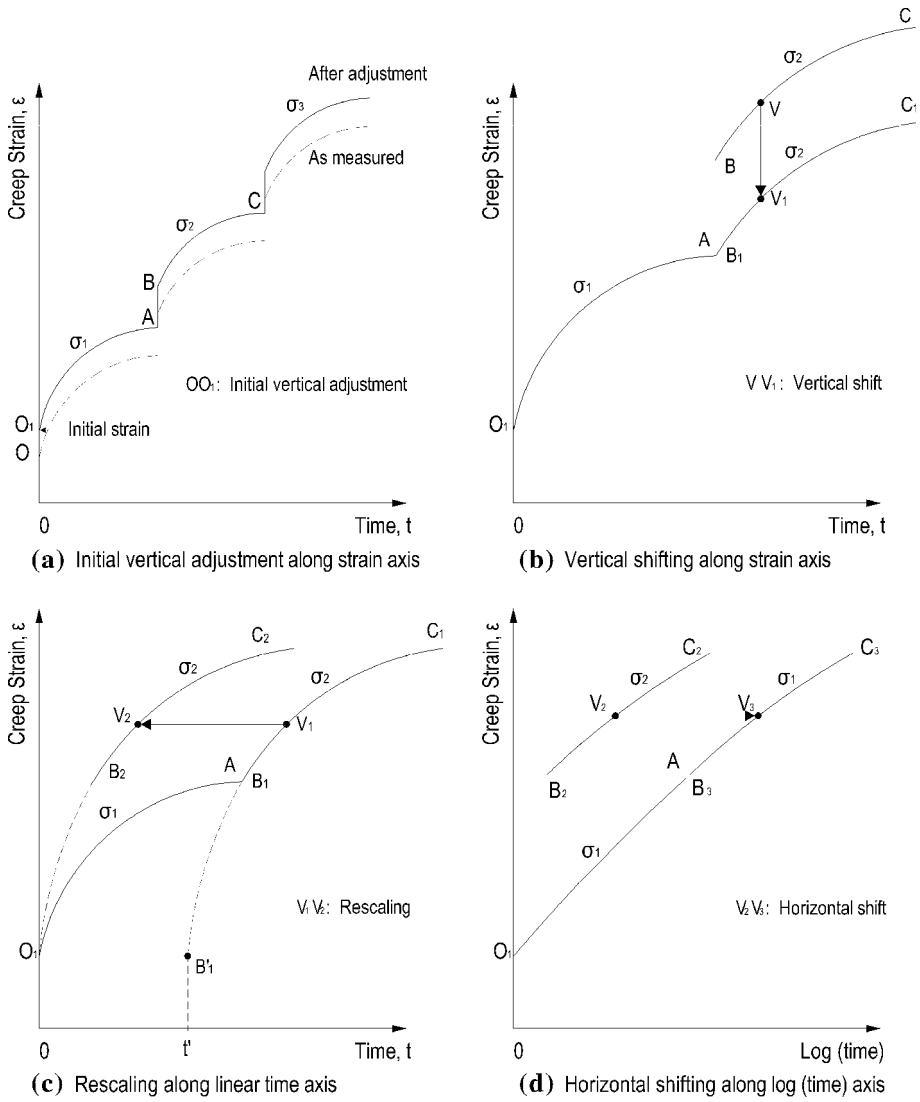

Fig. 3 SSM procedure in schematic diagrams

separate these different components, which is done in Fig. 3c. The curve B_1C_1 is shifted to the left, but allowance has to be made for the fact that this curve did not start with zero creep strain. Instead, the curve B_1C_1 is extrapolated to B_1' at time t', which is the point where it would have started if it had been carried out on a previously unloaded yarn. This process is known as rescaling and takes the form of a horizontal shift along the linear time axis of each creep curve at higher stress levels. The breaking down of the SSM curve into a set of rescaled creep curves, each of which would have been obtained from TSSP tests, is valid according to the Boltzmann's superposition principle.

A first estimate of t' at each stress level can be obtained following the above procedure (either graphically or numerically), but this is subjective. A more accurate determination is made numerically in combination with the horizontal shift, described in the next Section.

Horizontal shift

The result of rescaling is a series of curves, each of which represents part of a creep curve that would have been obtained from tests on different yarns at different stresses. They are thus the same as those that could have been obtained from separate TSSP tests. They must be *shifted* along the logarithmic time axis to obtain the creep master curve at a reference stress σ_R.

The magnitude of this *horizontal shift* is a function of stress and is similar in principle to the shift in TTSP testing where tests are carried out at different temperatures and the shift is a function of temperature. Two relationships have been developed to determine the effect of stress on the rate of creep, and hence on the required shift; these are based on: (1) the Eyring equation and (2) the modified WLF (Williams–Landel–Ferry) equation.

The choice between these two approaches depends on whether the temperature applied is below or above the glass transition temperature T_g [16]. Since aramids in general and Kevlar 49 in particular are highly crystalline polymers which display no glass transition temperature [28], it is expected to follow the Eyring equation, whose general form is:

$$k = \frac{k_B T}{h} e^{-\frac{\Delta G}{RT}} \quad (1)$$

ΔG is the Gibbs free energy of activation, k_B is Boltzmann's constant, h is Plancks's constant, R is the universal gas constant and T is the absolute temperature.

This leads to the following strain rate relationship [16]:

$$\dot{\varepsilon} = \dot{\varepsilon}_0 e^{-\frac{U}{RT}} \cdot e^{\frac{N_A V^* \sigma}{RT}} \quad (2)$$

where V^* is the stress coefficient and is referred to as the activation volume since it has dimensions L^3, U is the activation energy, N_A is the Avogadro constant and T is the absolute temperature. This derivation assumes that the activation volume is a constant, which can be checked later from the test results.

Equation 2 can be rearranged by comparing the ratio of strain rate $\dot{\varepsilon}_1$, at stress level σ_1, to strain rate $\dot{\varepsilon}_2$, at stress level σ_2, both measured at the same temperature T, as follows:

$$\ln\left(\frac{\dot{\varepsilon}_1}{\dot{\varepsilon}_2}\right) = \frac{V^*}{kT}(\sigma_1 - \sigma_2) \Rightarrow \log(\alpha_\sigma) = \frac{V^*}{2.30kT}(\sigma - \sigma_R) \quad (3)$$

The shifting factor α_σ is the ratio between the time for a viscoelastic process to proceed at an arbitrary stress and the time for the same process to proceed at a reference stress:

$$\varepsilon_R(\sigma_R, t) = \varepsilon\left(\sigma, \frac{t}{\alpha_\sigma}\right) \quad (4)$$

where ε_R is the strain at the reference stress level σ_R, t is time, ε is the strain at the elevated stress level σ.

Both the rescaling and the logarithmic shifting can be done graphically but it is better to follow a numerical procedure at each stress step so that a sufficiently smooth creep master curve is produced (Fig. 3c, d). This will allow the rescaling and shift factors to be determined from the test results, and the corresponding activation volume to be determined. The consistency of these values will in itself be a test of the validity of the method.

The master curve should be independent of the sequence of steps used in its determination. Thus, another check on the validity of the method is to compare the master curves produced using different stress steps, and the rupture times predicted should be consistent with acceptable accuracy. A test procedure was thus planned to cover many different stress sequences.

Materials and experimental set-up

Kevlar 49 yarns, available in reel form, were used for all tests. The cross-sectional area (A) of the yarns, after removing moisture, was found to be 0.17497 mm^2. The average breaking load (ABL) was found to be 445 N (from 20 specimens) which is equivalent to a breaking stress of 2.54 GPa. All values obtained are in agreement with the literature [29]. All subsequent stress levels will be expressed as a percentage of this ABL. Before testing, the yarn reels were kept at constant room temperature (25 °C) and humidity (50% relative humidity), placed in a black polythene bags inside a box to protect them from ultra violet light.

All the testing was carried out in an Instron test machine equipped with a 1 kN load cell. The yarn was clamped at both ends by wrapping it around spindle clamps that were attached to the testing machine by means of Invar bars (Fig. 4). The same apparatus was used to carry out SIM and TTSP creep tests, which require the use of elevated temperatures (up to 200 °C), so the clamps gripped the yarn a Thermocenter-Salvis Lab oven. Two holes were made in the top and bottom of the oven and the clamps with the yarn were fully inside the oven; the holes were

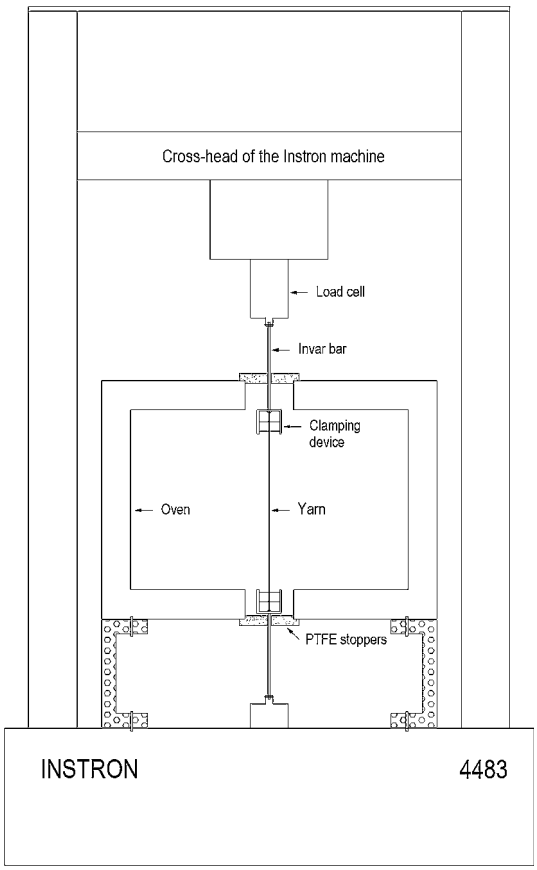

Fig. 4 Schematic drawing of testing apparatus and instrumentation

covered with stoppers made of PTFE to prevent heat loss. For the SSM tests the programmable oven was used to hold the temperature at 25 °C inside a room that was held at 21 °C.

A mechanical strain gauge was used in the tensile tests to measure the strain of the yarn. The mechanical strain gauge was made of spring steel. PTFE coated wires and high temperature electrical strain gauges were used so that it could be used with accuracy up to 205 °C. Before testing, the mechanical strain gauge had to be calibrated at various temperatures (described in detail in Giannopoulos and Burgoyne [30]). In all SSM tests, the overall extension is measured by a displacement transducer attached to the top cross-head, the tensile load is measured by a load cell and the temperature is measured by a thermo-couple. All mentioned data are recorded by a data logger at user-defined intervals or when a sudden change occurred.

The yarn was gripped by being wrapped around a spindle and then fixed by a grip (Fig. 5). These grips ensured that failures took place in the body of the yarn between the clamps, and since they could be mass-produced were also used for creep, stress-relaxation and strength-retention tests. An extensive programme of tests was undertaken to determine the jaw effect (the equivalent length of yarn that is moving within the jaws), and also the amount of slack. The values found elsewhere [30] only apply to the particular set of jaws and the particular type of fibre used but the techniques are general in nature and can be applied to any similar testing arrangement and any similar material. All results are presented here after making due allowance for these effects.

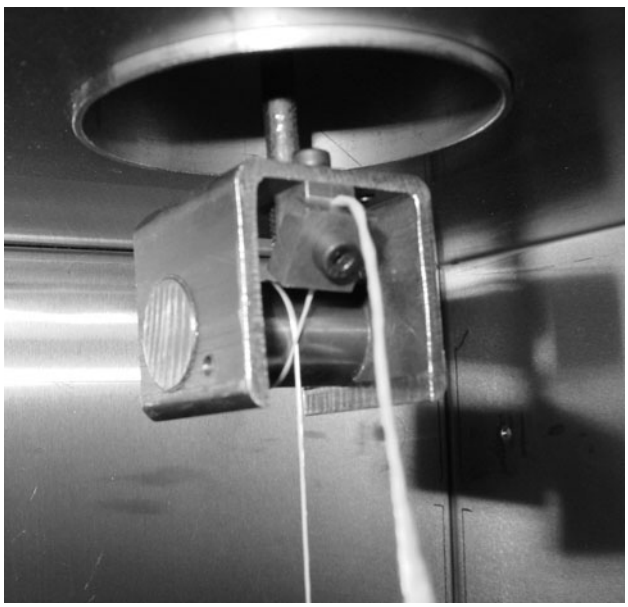

Fig. 5 Clamping device used in this study

Testing procedure

The yarn was first attached to the end grips. Before applying any load, a temperature of 25 °C was set and kept constant throughout each test. A starting reference load was initially applied to each specimen and three or four increasing load steps were followed. Each load step was chosen to last 5 h, except the final one which lasted until failure of the specimen. The steady state of creep is reached after about 1 h of testing and therefore 5 h of testing at each load step is satisfactory. The load cell was connected to a computer, where the desired load sequence was programmed. The load jump from one load level to the next was carried out in the shortest time possible, so creep that takes place during the load step itself can be ignored.

The above procedure was followed in each test with a different starting reference load: 50, 55, 60, 65, 70 and 75% of ABL, using four or five different load sequences. Each test was repeated; the two results are shown in pairs of columns in the tables. Details of all SSM tests carried out are given in Tables 1, 2, 3, 4, 5, 6. Each test is identified by a test label, e.g. SSM-75-02-01, where '75' denotes the starting reference load level, '02' denotes the test number and '01' denotes the repetition of the test.

Results and discussion

Detailed results are presented below for one test (SSM-75-01-01) to show how the method is applied, followed by a summary of all the results. The test readings monitored throughout each SSM test were used to produce plots of specimen elongation (Δl) versus time (t). These curves were then converted to strain versus time curves (Fig. 6) taking into account of the jaw effect (l_{jaw}) and the initial slack (s).

Table 1 SSM tests and shifting factors at starting ref. load 50% ABL

Test label	Load sequence (% ABL)	Time (h)		Rescaling factor r (h)		Shift factor log (α_σ)	
SSM-50-01-01	50	5	*5*	0.00	*0.00*	0.00	*0.00*
SSM-50-01-02	55	5	*5*	4.60	*4.56*	1.35	*1.30*
	60	5	*5*	9.54	*9.55*	2.60	*2.62*
	65	5	*5*	14.42	*14.22*	3.85	*3.82*
	80	1.6	*2.6*	20.19	*20.15*	6.90	*6.30*
SSM-50-02-01	50	5	*5*	0.00	*0.00*	0.00	*0.00*
SSM-50-02-02	60	5	*5*	4.90	*4.80*	1.74	*1.46*
	65	5	*5*	9.73	*9.80*	3.37	*3.01*
	70	5	*5*	14.75	*14.90*	4.80	*4.50*
	80	0.7	*2*	20.06	*20.08*	6.57	*6.45*

Table 2 SSM tests and shifting factors at starting ref. load 55% ABL

Test label	Load sequence (% ABL)	Time (h)		Rescaling factor r (h)		Shift factor log (α_σ)	
SSM-55-01-01	55	5	*5*	0.00	0.00	0.00	0.00
SSM-55-01-02	60	5	*5*	4.57	4.84	1.58	1.74
	65	5	*5*	9.80	9.73	3.18	3.24
	75	5	*5*	14.93	14.94	4.93	4.82
	80	1.3	*1.2*	19.56	19.70	6.21	5.99
SSM-55-02-01	55	5	*5*	0.00	0.00	0.00	0.00
SSM-55-02-02	65	5	*5*	5.04	4.99	2.41	2.48
	70	5	*5*	9.78	9.55	3.93	3.98
	75	6.8	*6.9*	14.68	14.68	5.32	5.39

Table 3 SSM tests and shifting factors at starting ref. load 60% ABL

Test label	Load sequence (% ABL)	Time (h)		Rescaling factor r (h)		Shift factor log (α_σ)	
SSM-60-01-01	60	5	*5*	0.00	*0.00*	0.00	*0.00*
SSM-60-01-02	65	5	*5*	4.79	*4.77*	1.20	*1.70*
	70	5	*5*	9.79	*9.78*	2.65	*3.12*
	75	5	*5*	14.87	*14.40*	3.97	*4.20*
	80	3	*7.2*	19.72	*19.51*	5.12	*5.20*
SSM-60-02-01	60	5	*5*	0.00	*0.00*	0.00	*0.00*
SSM-60-02-02	70	5	*5*	5.01	*5.02*	2.00	*2.00*
	75	5	*5*	9.86	*9.89*	3.55	*3.43*
	80	5	*5*	14.73	*14.95*	4.67	*5.08*
	82.5	2.3	*1.2*	18.50	*18.01*	5.20	*5.51*

Table 4 SSM tests and shifting factors at starting ref. load 65% ABL

Test label	Load sequence (% ABL)	Time (h)		Rescaling factor r (h)		Shift factor log (α_σ)	
SSM-65-01-01	65	5	*5*	0.00	*0.00*	0.00	*0.00*
SSM-65-01-02	70	5	*5*	4.23	*4.42*	1.16	*1.24*
	75	5	*5*	9.45	*9.75*	2.54	*2.80*
	80	14.6	*14.5*	14.68	*14.71*	3.98	*3.95*
SSM-65-02-01	65	5	*5*	0.00	*0.00*	0.00	*0.00*
SSM-65-02-02	75	5	*5*	4.89	*4.95*	2.06	*1.99*
	77.5	5	*5*	9.15	*9.45*	3.31	*3.19*
	80	5.8	*6.5*	14.18	*14.34*	4.30	*4.26*

Table 5 SSM tests and shifting factors at starting ref. load 70% ABL

Test label	Load sequence (% ABL)	Time (h)		Rescaling factor r (h)		Shift factor log (α_σ)	
SSM-70-01-01	70	5	*5*	0.00	*0.00*	0.00	*0.00*
SSM-70-01-02	75	5	*5*	4.50	*4.50*	1.39	*1.36*
	77.5	5	*5*	9.28	*9.28*	2.56	*2.46*
	80	5	*5*	13.75	*13.78*	3.39	*3.25*
	82.5	0.8	*0.7*	18.43	*18.47*	4.18	*3.84*
SSM-70-02-01	70	5	*5*	0.00	*0.00*	0.00	*0.00*
SSM-70-02-02	72.5	5	*5*	4.50	*4.07*	1.15	*0.93*
	75	5	*5*	9.51	*9.06*	2.20	*1.99*
	77.5	5	*5*	14.30	*13.61*	3.18	*2.84*
	82.5	3	*1.1*	19.30	*19.14*	4.19	*3.91*

Table 6 SSM tests and shifting factors at starting ref. load 75% ABL

Test label	Load sequence (% ABL)	Time (h)		Rescaling factor r (h)		Shift factor log (α_σ)	
SSM-75-01-01	75	5	*5*	0.00	*0.00*	0.00	*0.00*
SSM-75-01-02	77.5	5	*5*	3.52	*3.41*	0.69	*0.65*
	80	5	*5*	8.63	*8.68*	1.53	*1.48*
	82.5	3.9	*2.0*	13.84	*14.30*	2.40	*2.49*
SSM-75-02-01	75	5	*5*	0.00	*0.00*	0.00	*0.00*
SSM-75-02-02	77.5	5	*5*	3.50	*3.52*	0.71	*0.79*
	80	8.2	*8.3*	8.51	*8.64*	1.45	*1.67*

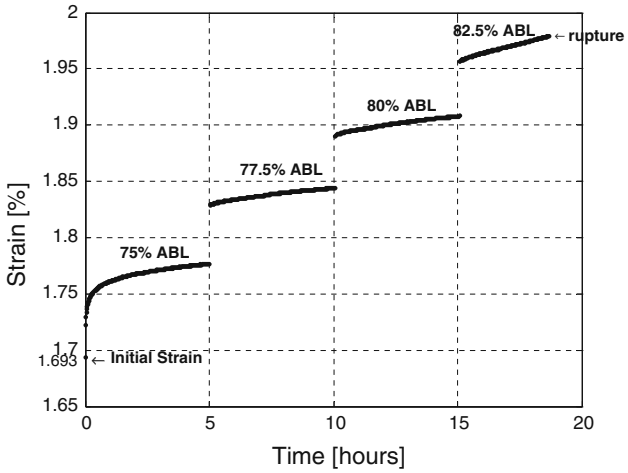

Fig. 6 Strain versus time curve of SSM-75-01-01 after the initial vertical adjustment

For Kevlar 49 the mean slack was found to be 0.42 mm and jaw effect meant that the effective length of fibre was found to be 140 mm longer than the nominal gauge length [30]. After applying the initial vertical adjustment, the result is a strain versus time plot (Fig. 6).

An increase of strain is observed in each stress jump of Fig. 6. This is shown more clearly in Fig. 7 where an enlarged portion of the curve is given around the second stress jump (77.5–80% ABL). The as-measured strain versus time curve of SSM-75-01-01 given in Fig. 6 is

adjusted vertically to remove the elastic strain, so that the final master curve is a purely creep curve (Fig. 8).

Each part of the curve of Fig. 8, corresponding to a different stress level, has to be rescaled by horizontal shifting in order to take into account the stress history of the specimen and to form a creep master curve. In order to obtain a smooth master curve, an iterative process was adopted. A third order polynomial was fitted to the rescaled and shifting curves to cover the period from 1 h before to 1 h after the stress step. The error between the actual strain and this polynomial were then calculated, and these were minimised by adjusting the rescaling factor (r measured in hours) and the horizontal shift factor log (α_σ).

The rescaling factor and shift factor that resulted for the load sequence of SSM-75-01-01 are given in Table 6. Using the rescaling factors the individual creep curves are produced (Fig. 9). These are assumed to be parts of the creep curves that could have been obtained from TSSP tests. Then, using the horizontal shifting factors, the final master curve is produced (Fig. 10). The very last point of this curve corresponds to the creep–rupture point of the specimen. For this test the rupture time is $10^{3.084}$ h = 50 days = 0.139 years.

The above procedure is followed at all load levels: 50, 55, 60, 65, 70 and 75% ABL. All rescaling factors and horizontal shifts for all tests are shown in Tables 1, 2, 3, 4, 5, 6 and the resulting master curves from all tests are shown together in Fig. 11 (black lines). Examining the SSM master curves at each load level, which resulted from four tests with different stress sequences, it is noticed that they match both in form and position with some experimental scatter. From all curves, it can be seen that creep strain values increase almost linearly with logarithmic time until shortly before failure.

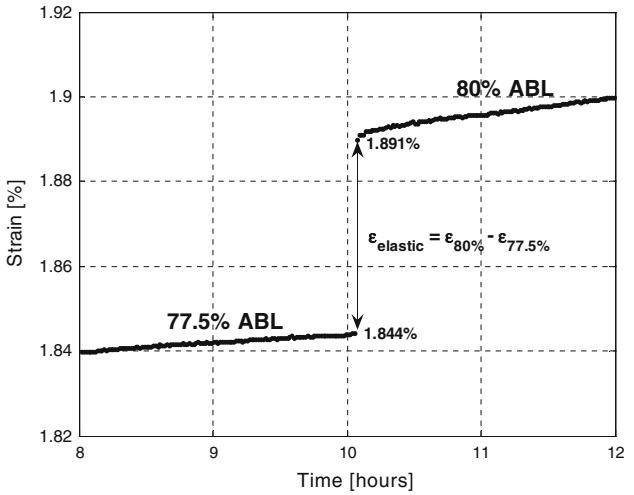

Fig. 7 Strain versus time curve at the stress jump 77.5–80% ABL of SIM-75-01-01

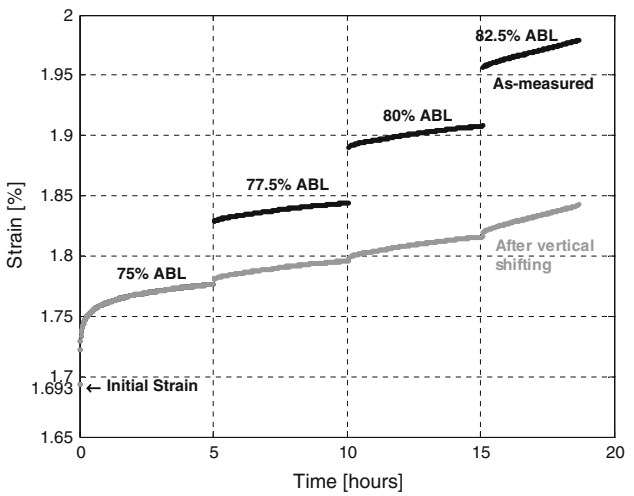

Fig. 8 Strain versus time curves as measured and after vertical shifting of SSM-75-01-01

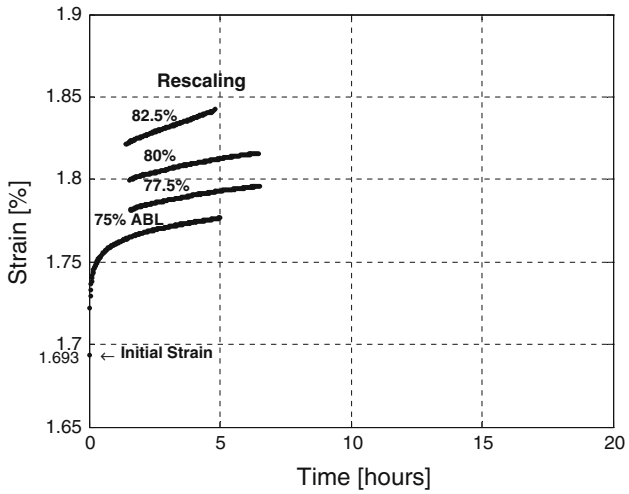

Fig. 9 Individual creep curves after rescaling of SSM-75-01-01

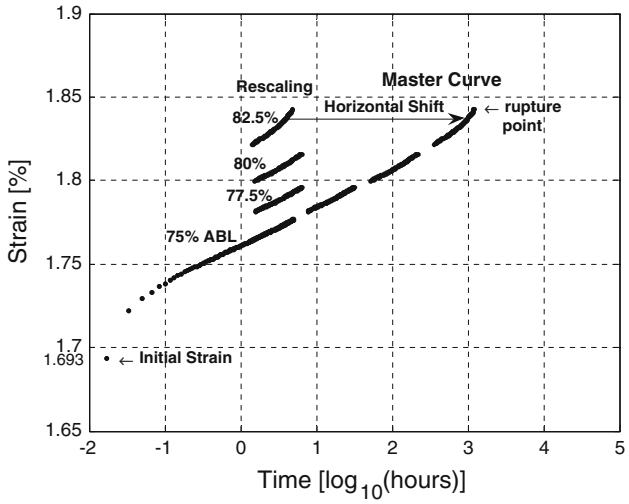

Fig. 10 Individual creep curves after rescaling and master curve after horizontal shifting of SSM-75-01-01

Validating the SSM method

A series of conventional creep tests (CCT) under constant temperature (25 °C) and humidity (50% RH) have been performed to check the validity of this method for Kevlar 49 [4]. The tests covered a wide stress spectrum (10–80% ABL) and lasted up to 1 year. The creep curves (grey lines) match reasonably closely with the corresponding SSM master curves (black lines), as can be seen in Fig. 11; the comparison is for only 1 year, which is the period of conventional testing. As far as can be ascertained, no creep data for such a long period of time under steady conditions has ever been reported in the past for Kevlar 49.

Comparison of the creep master curves obtained from the well-established SIM and the new SSM (Fig. 12) also show close matching between corresponding curves for Kevlar 49 for the whole life time, except for the curves at 50% ABL. In SIM testing, steep temperature jumps are required to reach the high temperature levels for failure to occur within 25 h at 50% ABL; this might affect the smoothness of the SIM master curve [31].

A typical SSM master curve (SSM-75-01-01) plotted on a linear time scale is given in Fig. 13. It can be observed that the shape of this curve is in general agreement with those found from conventional creep tests on parallel-lay aramid ropes, at various load levels (25–82% NBL), carried out by Chambers [12] and Guimaraes [1]. The general form of those curves is shown in Fig. 14. The curve is divided into three regions corresponding to primary, secondary and tertiary creep. The initial very fast creep rate reduces during the primary phase and is constant during the secondary phase. During the tertiary phase, the rate again increases leading to failure. The shape of this curve is a reflection of bundle effects, but since it is present at the size

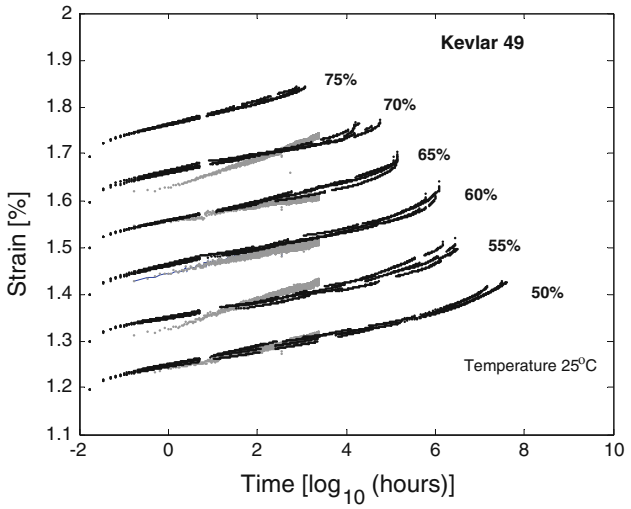

Fig. 11 SSM master curves (*black*) and conv. creep curves (*grey*) for Kevlar 49

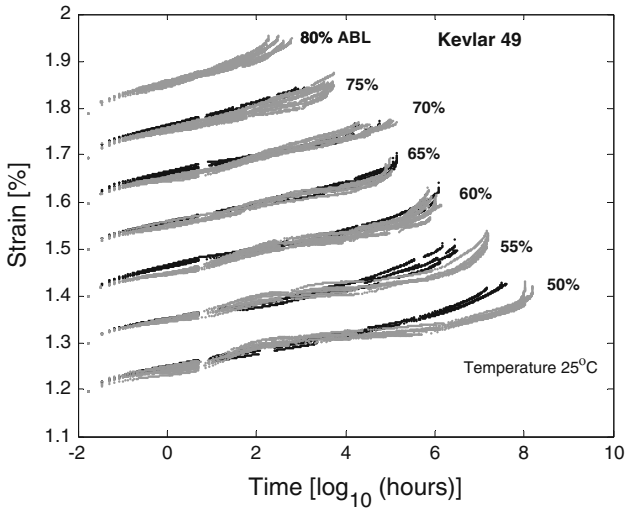

Fig. 12 All SSM (*black*) and SIM (*grey*) master curves for Kevlar 49

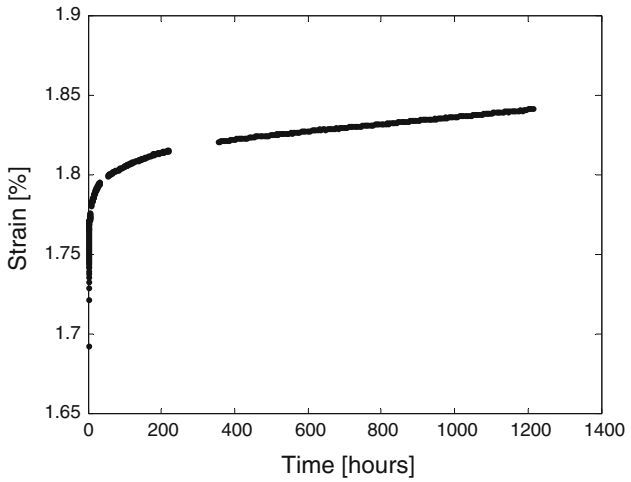

Fig. 13 A typical SSM master curve (SSM-75-01-01) in linear time scale

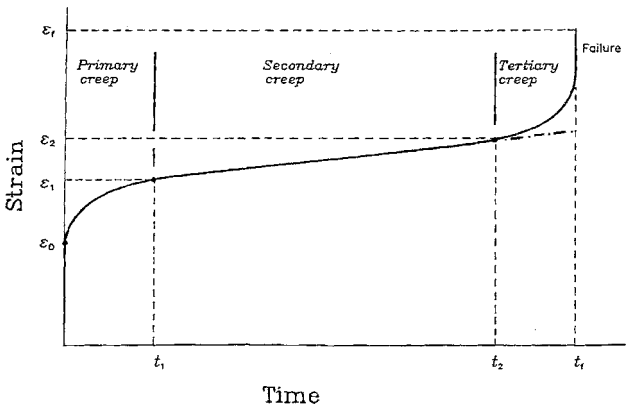

Fig. 14 Schematic creep curve [1]

of the yarn samples its form can be regarded as typical. All SSM curves in this study show these three distinct creep regions, apart from some tests such as SSM-75-01-01 where the tertiary phase is absent.

Activation volume

The creep data from all the SSM tests can be used to check the validity of the Eyring equation for Kevlar 49 yarns (Eq. 3). The horizontal shifting needed from each accelerating stress to produce the master curve at the reference stress is related to the activation volume. Figure 15 shows a typical plot of the shift factors (calculated numerically to produce smooth master curves) for yarns tested with an initial stress (and reference stress) of 50% ABL. The fact that the data points on this plot lie close to a straight line, with a small experimental scatter, shows that the same creep mechanism is operative for each load sequence, which validates the use of the superposition theory in adding creep curves with different load sequences to produce the creep master curve that underlies the SSM procedure.

The slope of the line on Fig. 15 is equal to $V^*/(2.30kT)$, where V^* is the activation volume and k is Boltzmann's constant ($=1.38 \times 10^{-23}$ J K^{-1}) and T is the temperature. The resulting values of V^* at different starting reference loads, given in Table 7, show an increase with the increase of the applied load. This implies a relationship between activation volume and stress. According to transition state theory, activation volume V^* for a chemical process is interpreted as the difference between the partial molar volumes of the transition state and the sums of the partial volumes of the reactants at the same temperature and pressure [32]. A physical analogue would be that the products of the creep process occupy a larger volume than the original fibre. This may be consistent with the idea that the molecules are pulled apart during creep.

The variation of activation volume with reference stress is shown in Fig. 16, which is consistent with there being a linear relationship. This calls into question the original assumption, implicit in state theory and explicitly used earlier in the derivation of Eq. 3. If V^* varies with reference stress, why does it not vary with accelerating stress? Why then does the data shown in Fig. 15 give a straight line when a parabola would be expected if V^* varied linearly with stress. This is currently under investigation.

Limited data is reported in the literature for the activation volume for Kevlar 49. Slutsker [33] tested Kevlar 49 yarns and found a value of 0.150 nm^3. Bosman et al. [34] tested aramid fibres and found for 'standard' and 'annealed' fibres values of 0.100 and 0.138 nm^3, respectively. These values are of the same order as those obtained in this study.

Creep-rupture results

The final stage is to investigate the creep-rupture behaviour of Kevlar 49. All accelerated SSM tests at various load

Table 7 Activation volume at different reference loads for Kevlar 49

Reference load (% ABL)	Polynomial		Activation volume V* (nm^3)
	Slope a	Constant b	
50	0.22	−10.91	0.082
55	0.25	−13.27	0.091
60	0.24	−14.59	0.091
65	0.27	−17.61	0.100
70	0.32	−22.45	0.120
75	0.32	−24.17	0.120
ALL	0.24	−12.30	0.091

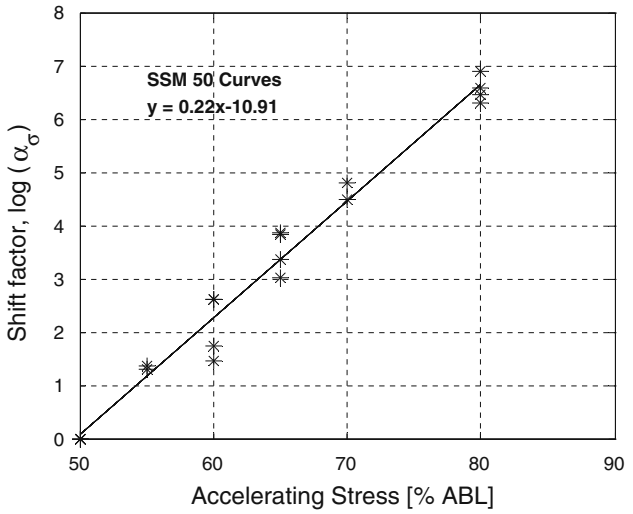

Fig. 15 A typical Eyring plot of SSM curves at starting reference load 50% ABL

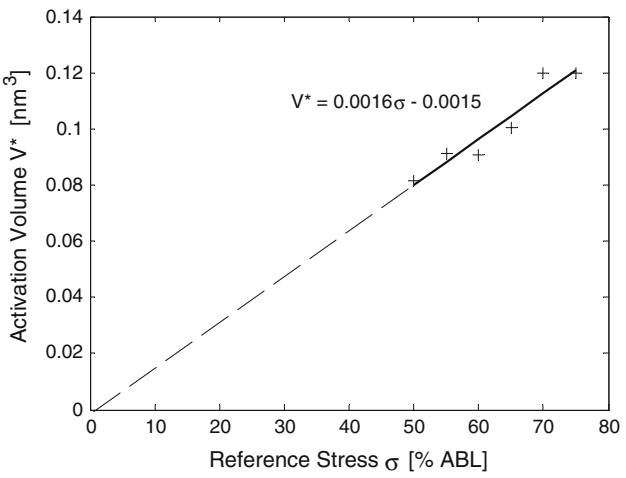

Fig. 16 Linear relationship between activation volume and reference stress

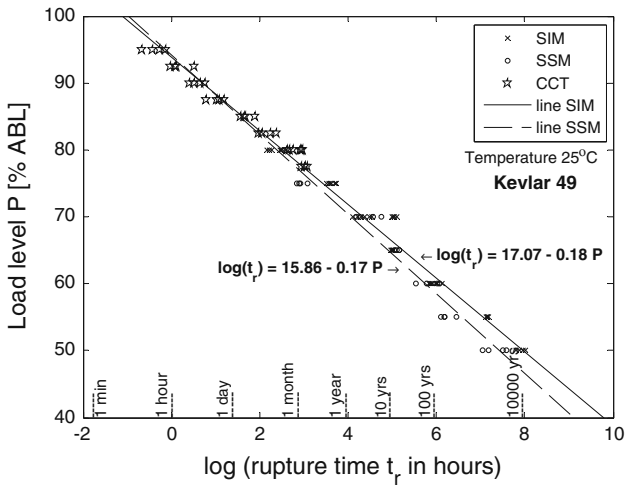

Fig. 17 Rupture times of SIM, SSM and CCT for Kevlar 49 yarns

levels were carried out until failure of the specimen (Fig. 11). The very last point of a master curve corresponds to the rupture time of the specimen at a constant temperature (25 °C). The creep-rupture-time values are plotted at various load levels (Fig. 17). It is observed that for load levels between 50 and 77.5% ABL there is a linear increase of the rupture logarithmic time with decreasing applied load, given by:

$$\log\,(t_r) = 15.86 - 0.17P \qquad (5)$$

The variation of the test data at all load levels about this line is small indicating the success of the SSM in deriving rupture times which by conventional creep tests would have required months or years.; a thorough study of the variation of the lifetime values is presented elsewhere [5]. CCT between 77.5 and 95% ABL and SIM tests between 50 and 80% ABL for Kevlar 49 are available [29] for comparison purposes with SSM tests and are shown all together in Fig. 17. The two fitted lines for SIM and SSM tests are also plotted and a good agreement is observed, which proves that the SSM technique is working well.

General discussion and conclusions

The SSM test, introduced here, has been shown to be a feasible method to predict the long-term creep and stress rupture behaviour of fibres. It has the advantage over SIM testing that the tests are carried out at one temperature, so no oven is needed.

The resulting creep and stress rupture curves are in good agreement with the conventional creep tests and accelerated SIM tests. However, the method relies on adjusting the fitting parameters to give a smooth master curve, which can be subjective, and it has been shown that the activation volume appears to vary with stress, whereas the activation energy that shows the effect of temperature appears to be constant. This needs to be the subject of future study.

Overall, the tests showed that the SSM technique offers a safe and quick route to the determination of the creep-rupture lifetime of high modulus fibres like aramids. Such data will be essential for their practical application in many civil engineering fields in the future.

References

1. Guimaraes GB (1988) Parallel-lay aramid ropes for use in structural engineering. University of London, London
2. Burgoyne, CJ (1992) In: Doran DK (ed) Construction materials reference book, Butterworths, Oxford
3. Gerritse A, Taerwe L (1999) In: Proceedings of the 4th international symposium on fiber reinforced polymer reinforcement for reinforced concrete structures, ACI SP-188
4. Giannopoulos IP (2009) Creep and creep-rupture behaviour of aramid fibres. University of Cambridge, Cambridge
5. Giannopoulos IP, Burgoyne CJ (2009) Struct Build 162(4):221
6. Chiao TT, Wells JE, Moore RL, Hamstad MA (1974) In: 3rd conference on composite materials: testing and design
7. Phoenix SL, Wu EM (1983) In: Hashin Z, Herakovich CT (eds) Mechanics of composites materials: recent advances, Pergamon Press, New York
8. Glaser RE, Moore RL, Chiao TT (1984) Compos Technol Rev 6(1):26
9. Wagner HD, Schwartz P, Phoenix SL (1986) J Mater Sci 21:1868. doi:10.1007/BF00547921
10. Wu HF, Phoenix SL, Schwartz P (1988) J Mater Sci 23:1851. doi:10.1007/BF01115731
11. Phoenix SL, Grimes-Ledesma L, Thesken JC, Murthy PLN (2006) In: Proceedings of the american society for composites, 21st annual technical conference, 17–20 Sep 2006, The University of Michigan-Dearborn, Dearborn
12. Chambers JJ (1986) Parallel-lay aramid ropes for use as tendons in prestressing concrete. University of London, London
13. Guimaraes GB, Burgoyne CJ (1992) J Mater Sci 27:2473. doi:10.1007/BF0110506
14. Yamaguchi T, Kato Y, Nishimura T, Uomoto T (1997) In: Proceedings of the 3rd international symposium on non-metallic reinforcement for concrete structures (FRPRCS-3), vol 2, Sapporo
15. Ando N, Matsukawa T, Hattori M, Mashima M (1997) In: Proceedings of the 3rd international symposium on non-metallic reinforcement for concrete structures (FRPRCS-3), vol 2, Sapporo
16. Ward IM, Sweeney J (2004) An introduction to the mechanical properties of solid polymers. Wiley, London
17. Thornton JS, Paulson JN, Sandri D (1998) In: Sixth international conference on geosynthetics, Atlanta
18. Alwis KGNC, Burgoyne CJ (2008) J Mater Sci 43(14):4789. doi:10.1007/s10853-008-2676-0
19. Lai J, Bakker A (1995) Polymer 36(1):93
20. Hadid M, Rechak S, Tati A (2004) Mater Sci Eng 385:54
21. Jazouli S, Luo W, Bremand F, Vu-Khanha T (2006) Key Eng Mater 340–341:1091
22. Ma CCM, Tai NH, Wu SH, Lin SH, Wu JF, Lin JM (1997) Composites B 28B:407
23. Luo W, Wang C (2007) Key Eng Mater 340–341:1091
24. Farquhar D, Mutrelle FM, Phoenix SL, Smith RL (1989) J Mater Sci 24:2151. doi:10.1007/BF02385436

25. Ericksen RH (1976) Composites 7:189
26. Ericksen RH (1985) Polymer 26:733
27. Alwis KGNC (2003) Accelerated testing for long-term stress-rupture behaviour of aramid fibres. University of Cambridge, Cambridge
28. Yang HH (1993) Kevlar aramid fiber. Wiley, Chichester
29. Du Pont EI (1991) Data manual for fibre optics and other cables. EI Du Pont de Nemours and Co (Inc.), Wilmington
30. Giannopoulos IP, Burgoyne CJ (2009) In: 16th Concrete Conference, Paphos, 21–23 Oct 2009
31. Giannopoulos IP, Burgoyne CJ (2008) In: 5th conference on advanced composite materials in bridges and structures (ACMBS-V) Paper 79, Winnipeg
32. Truhlar DG, Garrett BC, Klippenstein SJ (1996) J Phys Chem 100(31):12771
33. Slutsker AI (1989) Makromol Chem 27:207
34. Bosman M, Van der Zwaag S, Schenkels FAM (1995) J Mater Sci Lett 14:1440